Supplementary Information
Thorough investigation on the high-temperature polymorphism of dipentyl-perylenediimide: thermal expansion vs polymorphic transition.

Francesco Marin[a], Serena Tombolesi[a], Tommaso Salzillo*[,b], Omer Yaffe[b], Lucia Maini*[,a]

[a]Dipartimento di Chimica "G. Ciamician", via Selmi 2, Università di Bologna, 40126 Bologna, Italy

[b]Department of Chemical and Biological Physics, Weizmann Institute of Science, Herzl Street 234, 76100 Rehovot, Israel

Table of contents

Solubility

The solubility of PDI-C$_5$ in the solvents used in this work was extrapolated from its absorption spectra in a
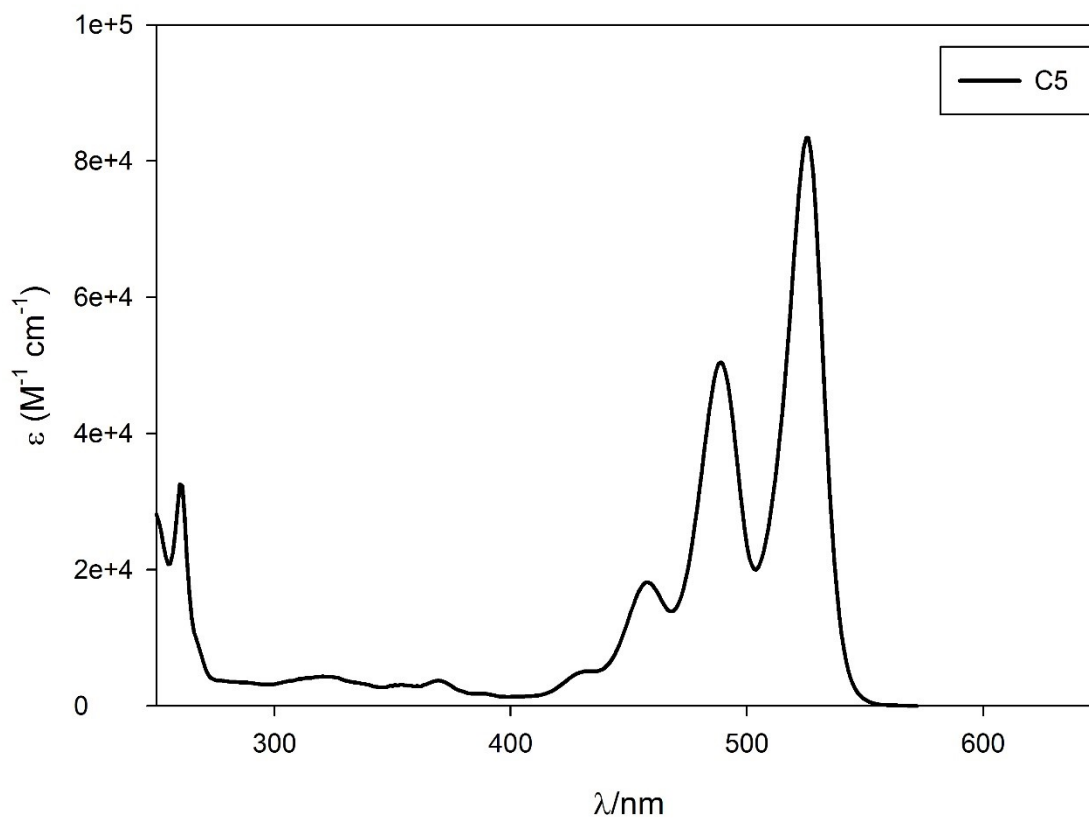
saturated solution.

Figure S1. Absorption spectra of PDI-C$_5$ in CHCl3 to determine the maximum solubility in the solvent. Concentration of PDI-C$_5$ in solution: C = $2.2 \times 10^{-5} M$.
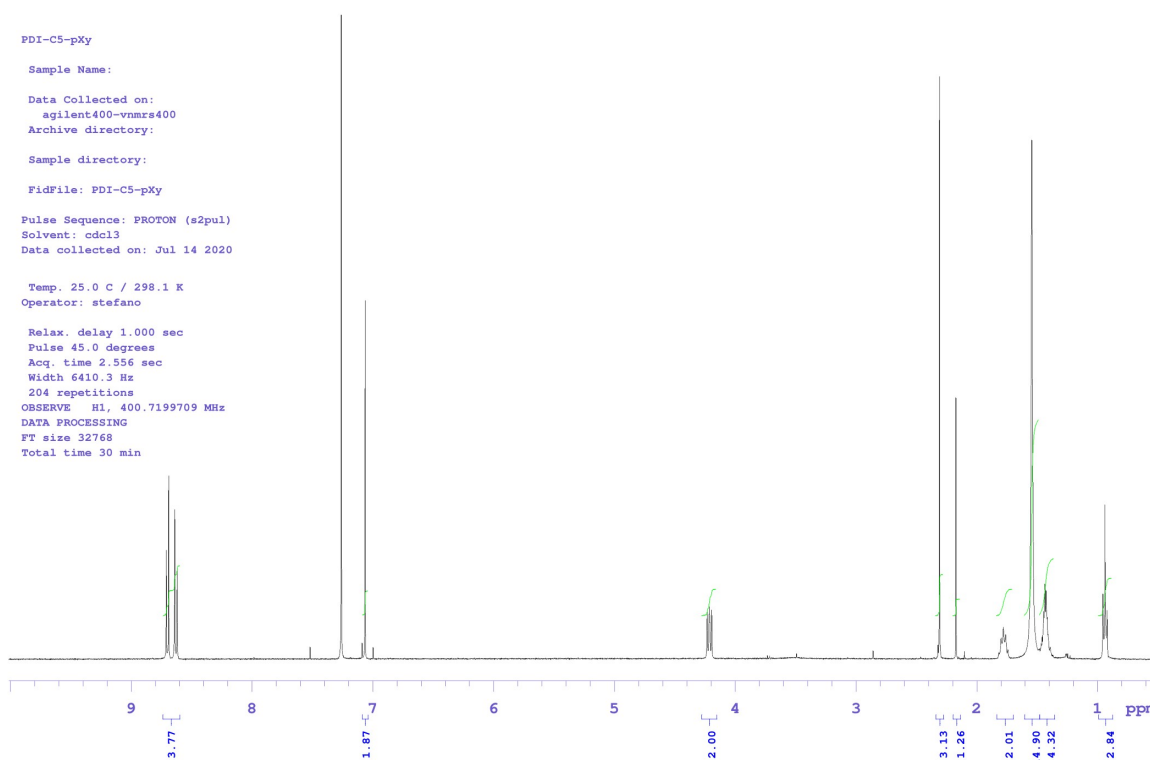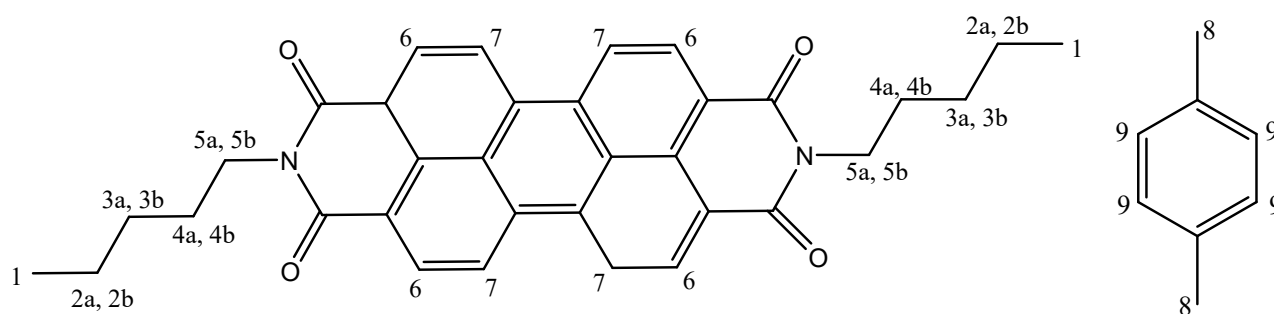
NMR Spectroscopy

PDI-C5-pXy

Sample Name:

Data Collected on:
  agilent400-vnmrs400
Archive directory:

Sample directory:

FidFile: PDI-C5-pXy

Pulse Sequence: PROTON (s2pul)
Solvent: cdcl3
Data collected on: Jul 14 2020

Temp. 25.0 C / 298.1 K
Operator: stefano

Relax. delay 1.000 sec
Pulse 45.0 degrees
Acq. time 2.556 sec
Width 6410.3 Hz
204 repetitions
OBSERVE H1, 400.7199709 MHz
DATA PROCESSING
FT size 32768
Total time 30 min

Figure S2. NMR spectra of PDI-C$_5$-pxy solvate form.

^{1}H-NMR (300 MHz, CDCl$_3$, 298K): δ 0.9 ppm (m, 6H, H1), 1.4-1.5 ppm (m, 8H, H2a-H2b-H3a-H3b), 1.8 ppm (m, 4H, H4a-H4b), 2.17 ppm (acetone used for washing crystals after filtering), 2.3 ppm (m, 6H, H8), 4.2 ppm (m, 4H, H5a-H5b), 7.0 ppm (m, 4H, H9), 7.26 ppm (hydrogen of CHCl$_3$ present in small quantity in the solvent), 8.6 ppm (m, 8H, H6-H7).
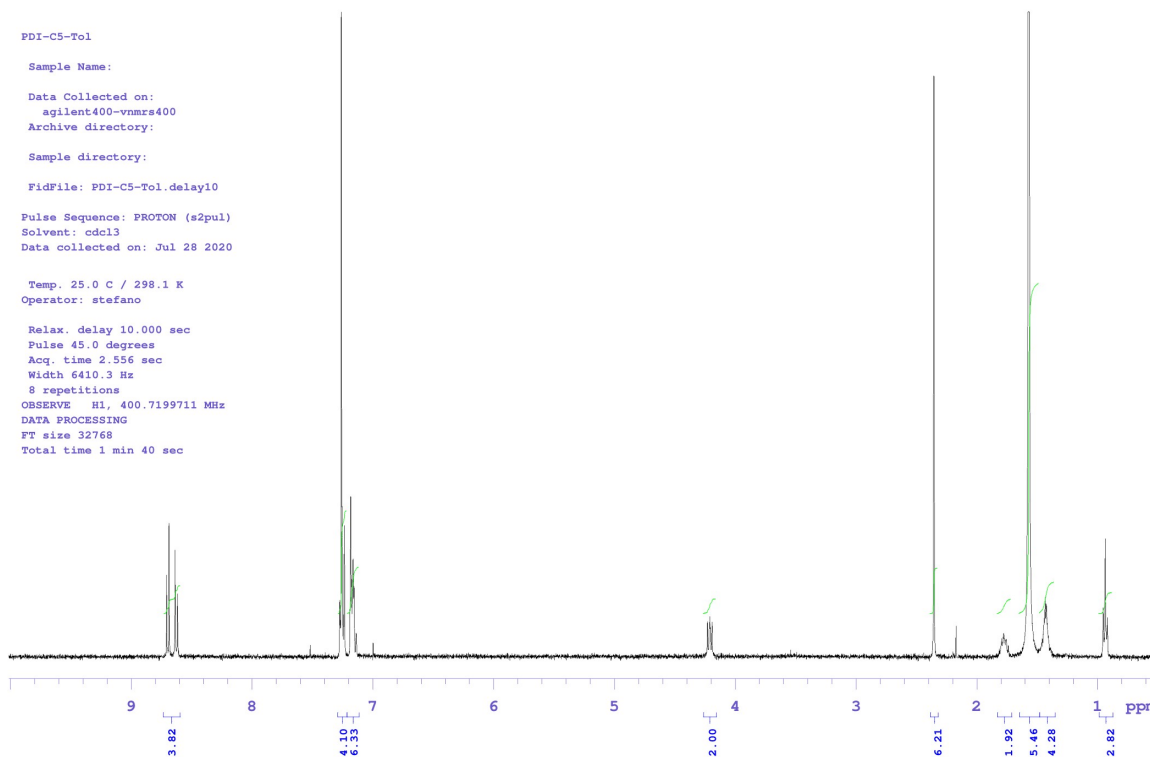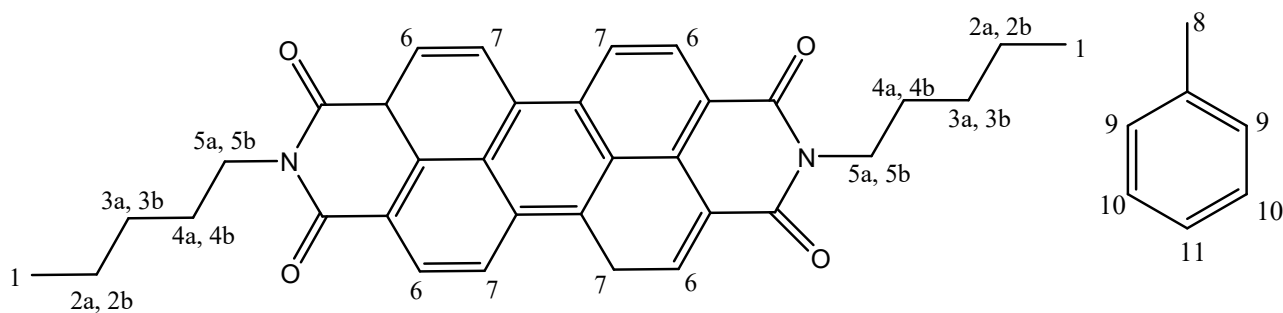
Figure S3. NMR spectra of PDI-C₅-tol solvate form.

^{1}H-NMR (300 MHz, CDCl₃, 298K): δ 0.9 ppm (m, 6H, H1), 1.4-1.6 ppm (m, 8H, H2a-H2b-H3a-H3b), 1.8 ppm (m, 4H, H4a-H4b), 2.17 ppm (acetone used for washing crystals after filtering), 2.3 ppm (m, 3H, H8), 4.2 ppm (m, 4H, H5a-H5b), 7.1-7.3 ppm (m, 5H, H9-H10-H11), 7.26 ppm (hydrogen of CHCl₃ present in small quantity in the solvent), 8.7 ppm (m, 8H, H6-H7).
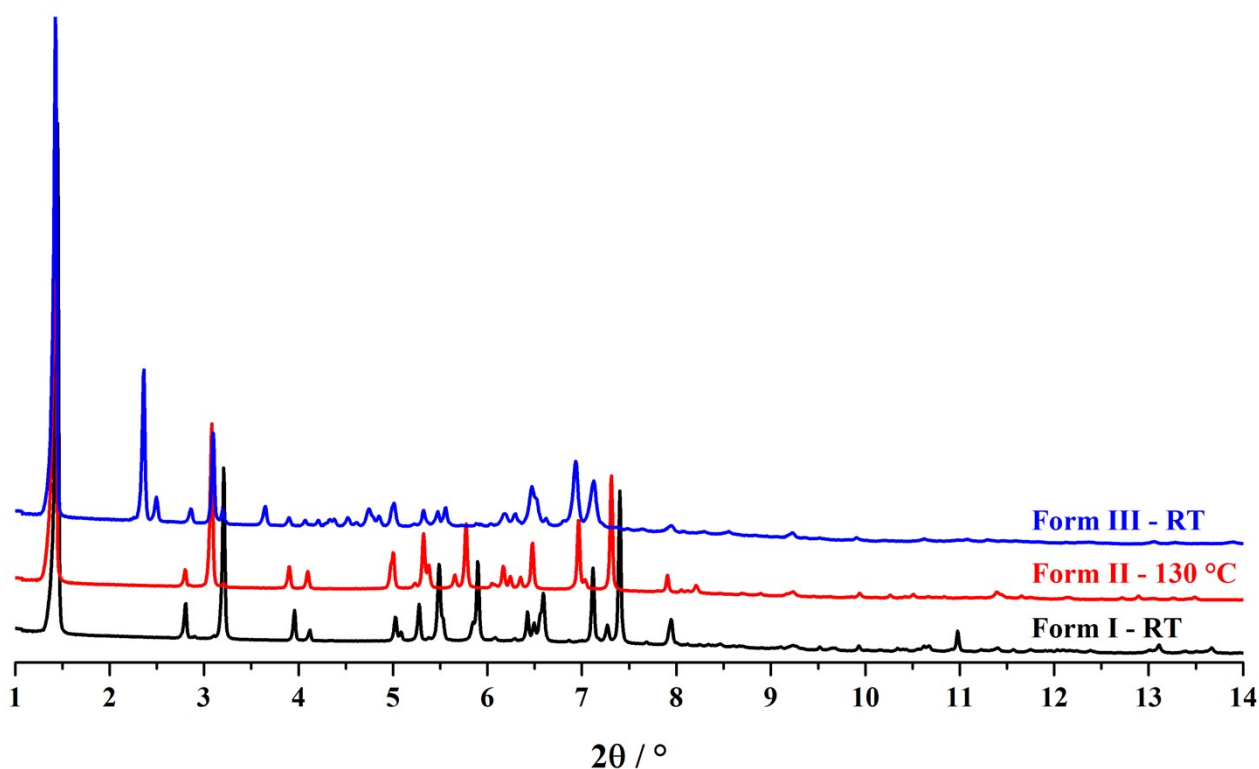
X-ray Crystallography

Figure S4. PXRD pattern (λ = 0.41235 Å) of the three PDI-C_5 crystal forms I (in black, collected at RT), II (in red, collected at 130 °C for structure solution) and III (in blue, collected at RT for structure solution).

The Rietveld refinement plot used to determine the crystal structures of form II and form III of PDI-C_5 from synchrotron powder data are reported. Form II crystal structure was determined at 131 °C, whereas form III crystal structure was determined at room temperature after cooling. Lamda and zero error were refined against the Si standard at RT. The background was described with Chubychev polynomial and the glass capillary modelled with 2 peaks at 2θ= 6.00° and 2θ= 7.79°. No correction for preferential orientation was applied.
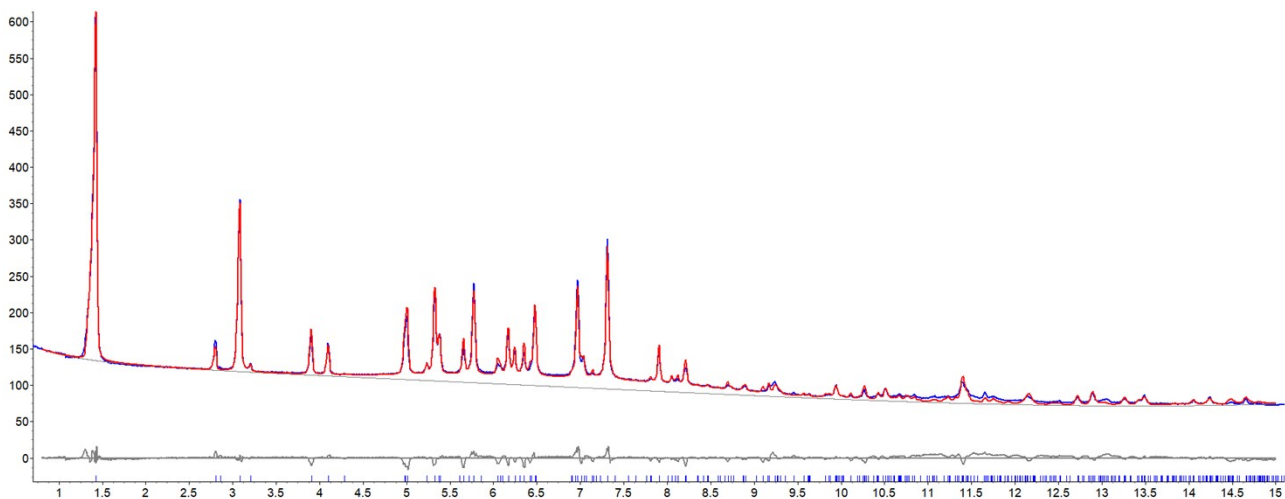
Figure S5. Rietveld refinement of form II at 131 °C. In blue is the experimental powder pattern, in red the calculated powder pattern and in grey is the difference pattern. Intensity is plotted in square root.

Figure S6. Rietveld refinement of form III at room temperature. In blue is the experimental powder pattern, in red the calculated powder pattern and in grey is the difference pattern. Intensity is plotted in square root.
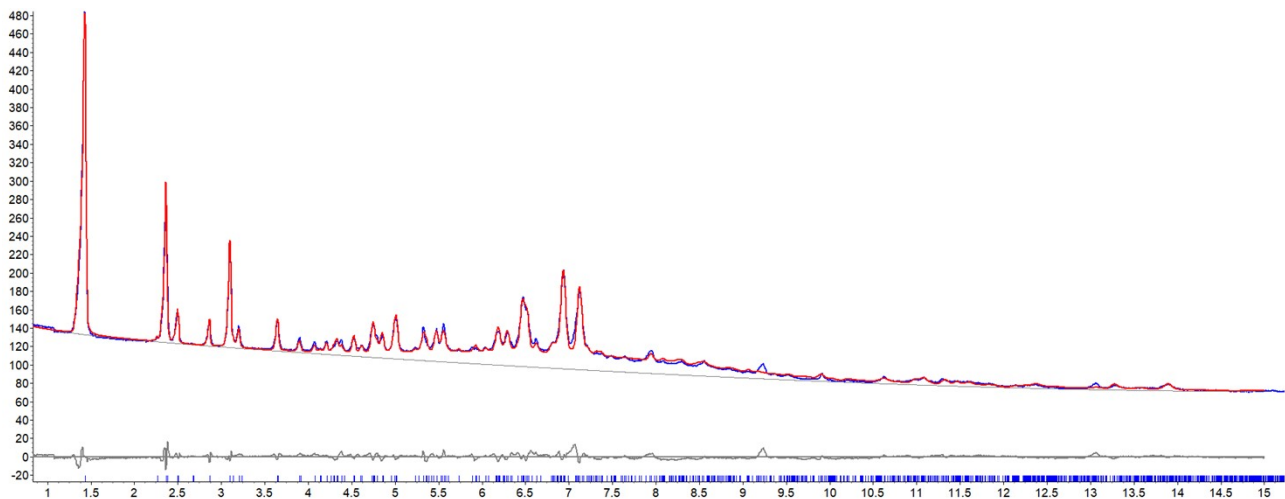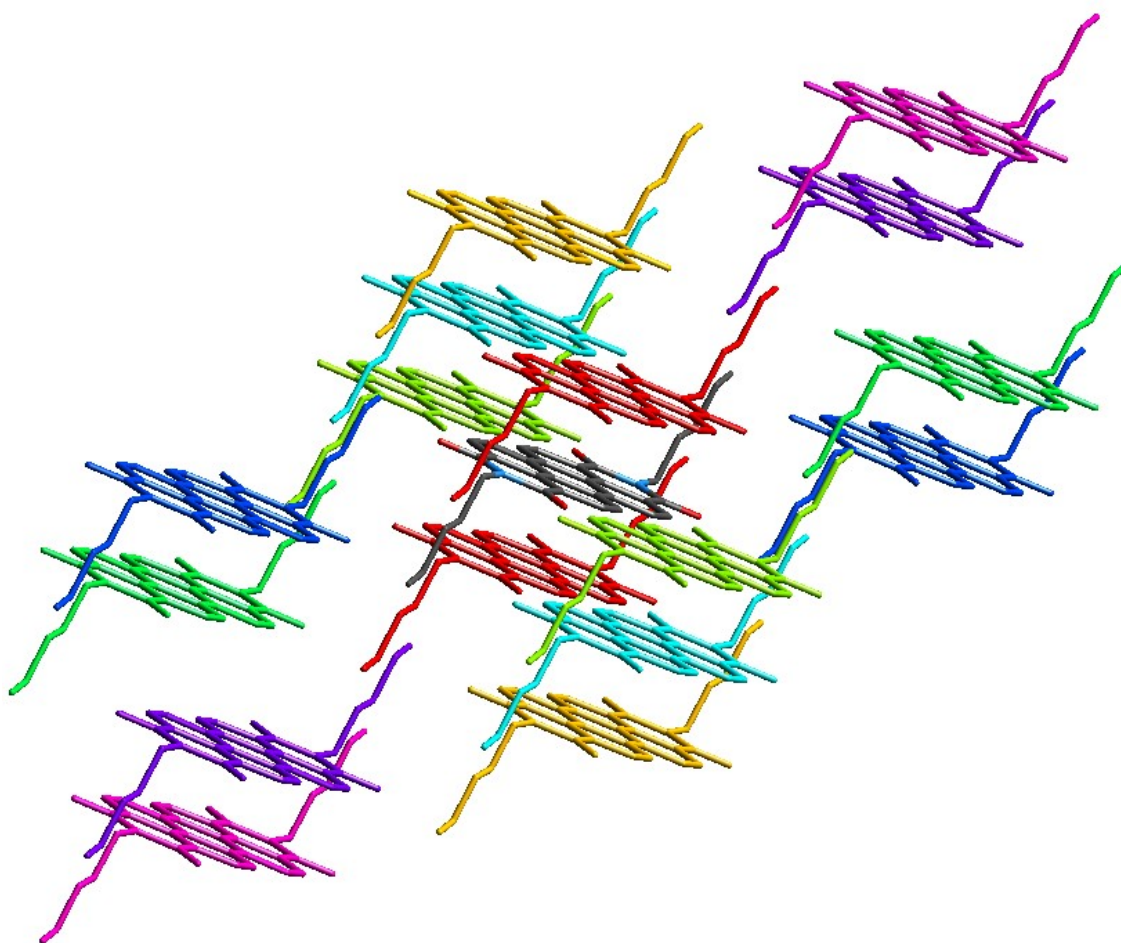
Energy Frameworks

Figure S7. View of the cluster of molecules of form I used for the interaction energies calculation. The central molecule is marked with the atom specific colours (C=grey; O=red; N=blue), the surrounding molecules are marked by an identification colour. Hydrogens are omitted for clarity.

Table 1. Interaction energies for PDI-C$_5$ form I (kJ/mol). The colours represent the corresponding molecule in Figure S7. Total energies are the sum of the four energy components, scaled appropriately (see

Table **2**)

Id. colour	N. molecules	Distance (Å)	E_ele	E_pol	E_dis	E_rep	E_tot
	2	4.75	-16.9	-2.3	-177.4	95.6	-115.0
	2	8.48	-1.2	-1.4	-16.4	2.5	-15.0
	2	12.02	-18.1	-4.7	-16.3	16.2	-26.8
	2	19.75	-2.0	-1.4	-22.4	9.9	-16.5
	2	9.25	-12.9	-6.4	-62.3	37.7	-49.4
	2	21.83	-0.5	-0.1	-10.2	4.4	-6.8
	2	26.09	-0.9	-0.0	-5.5	4.2	-3.2
	2	24.56	-0.2	-0.0	-2.4	0.6	-2.0

Table 2. Scale factors for the different contributions to calculate total energy for interaction energies.

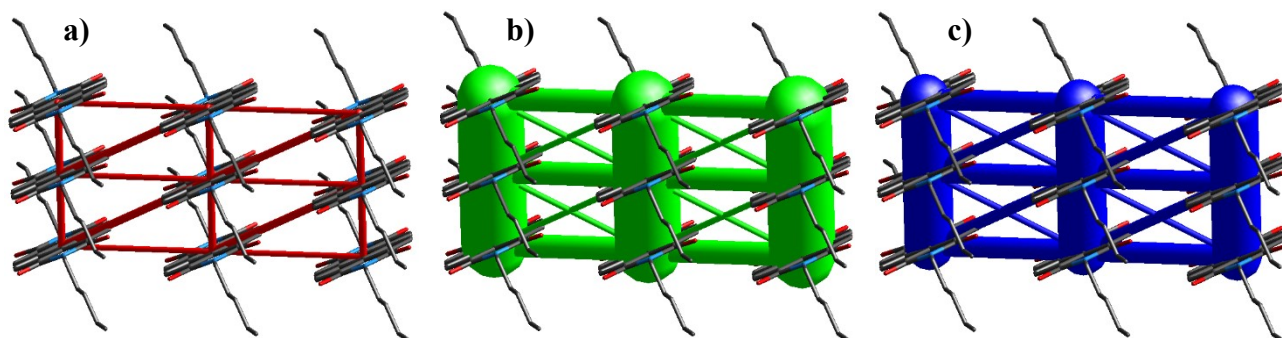| k_ele	k_pol	k_disp	k_rep
1.057	0.740	0.871	0.618

Figure S8. Graphic representation of the energy framework in PDI-C$_5$ form I calculated with CystalExplorer. The thickness of the lines is directly correlated with the intensity of the interaction. (a) electrostatic energy framework (red); (b) dispersion energy framework (green); (c) total energy framework (blue).
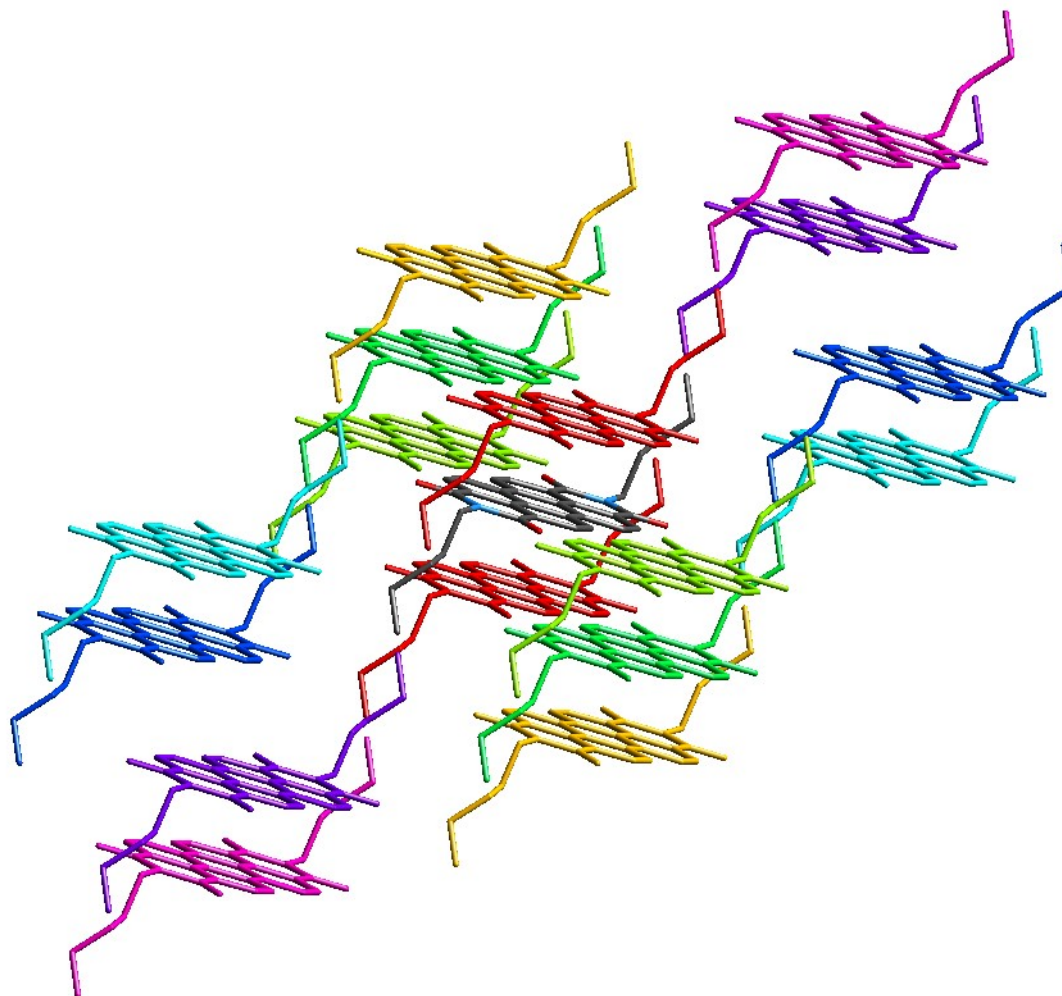
Figure S9. View of the cluster of molecules of form II used for the interaction energies calculation. The central molecule is marked with the atom specific colours (C=grey; O=red; N=blue), the surrounding molecules are marked by an identification colour. Hydrogens are omitted for clarity.

Table 3. Interaction energies for PDI-C$_5$ form II (kJ/mol). The colours represent the corresponding molecule in Figure S9. Total energies are the sum of the four energy components, scaled appropriately (see Table 2)

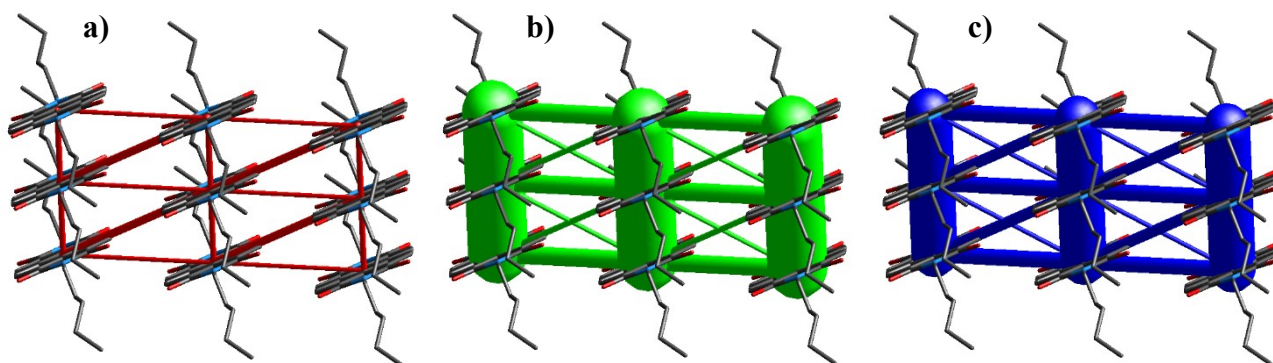| Id. colour	N. molecules	Distance (Å)	E_ele	E_pol	E_dis	E_rep	**E_tot**
	2	4.85	-13.5	-2.2	-164.8	78.2	-111.1
	2	8.53	-0.3	-1.3	-13.1	2.1	-11.3
	2	11.93	-18.7	-4.8	-16.5	16.3	-27.6
	2	9.17	-10.1	-5.0	-50.3	30.6	-39.2
	2	21.29	-0.6	-0.1	-8.5	2.0	-6.9
	2	19.23	-5.3	-1.4	-20.0	15.3	-14.6
	2	25.04	-2.3	-0.0	-6.7	8.3	-3.1
	2	23.58	-1.3	-0.0	-6.1	5.6	-3.3

Figure S10. Graphic representation of the energy framework in PDI-C$_5$ form II calculated with CystalExplorer. The thickness of the lines is directly correlated with the intensity of the interaction. (a) electrostatic energy framework (red); (b) dispersion energy framework (green); (c) total energy framework (blue).
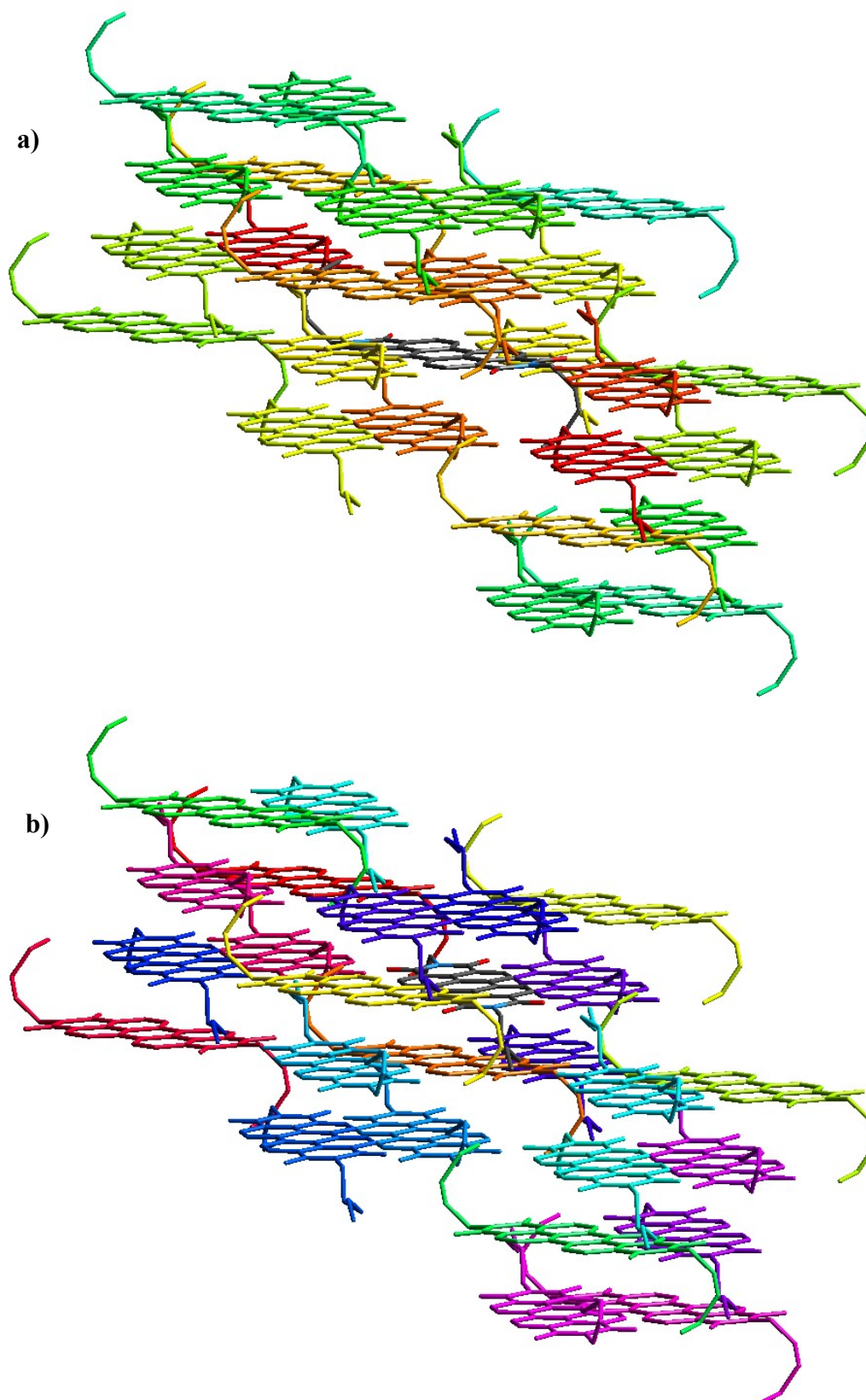
Figure S11. View of the cluster of molecules of form III used for the interaction energies calculation. The central molecule is marked with the atom specific colours (C=grey; O=red; N=blue), the surrounding molecules are marked by an identification colour. Hydrogens are omitted for clarity. (a) Central molecule is the one with alkyl chains in trans configuration; (b) Central molecule is the one with alkyl chains in cis configuration.

Table 4. Interaction energies for PDI-C$_5$ form III (kJ/mol), calculated respect to the molecule with alkyl chains in trans configuration. The colours represent the corresponding molecule in Figure S11a. Total energies are the sum of the four energy components, scaled appropriately (see

Table **2**).

Id. colour	N. molecules	Distance (Å)	E_ele	E_pol	E_dis	E_rep	E_tot
	2	24.10	-0.5	-0.0	-3.4	1.7	-2.5
	1	25.38	-0.1	-0.0	-0.2	0.0	-0.3
	2	3.63	-28.6	-6.4	-171.3	117.1	-111.8
	1	12.31	-0.9	-0.1	-1.4	0.0	-2.2
	2	22.96	-0.0	-0.0	-0.3	0.0	-0.3
	2	10.57	-17.1	-5.2	-39.8	36.3	-34.1
	2	10.82	-5.0	-2.1	-14.3	2.3	-17.8
	2	17.94	-9.5	-2.7	-19.9	30.4	-10.5
	2	19.51	-0.3	-0.1	-10.5	1.6	-8.6
	1	8.01	-0.0	-0.1	-6.7	0.0	-6.0
	1	14.75	-0.3	-0.0	-1.3	0.0	-1.5
	2	17.44	-0.7	-0.6	-8.3	2.3	-7.0
	2	22.35	-2.4	-0.0	-6.2	8.4	-2.7
	2	17.41	-0.3	-0.0	-5.6	0.4	-5.0
	1	11.62	1.2	-0.1	-1.6	0.0	-0.2

Table 5. Interaction energies for PDI-C$_5$ form III (kJ/mol), calculated respect to the molecule with alkyl chains in cis configuration. The colours represent the corresponding molecule in Figure S11b. Total energies are the sum of the four energy components, scaled appropriately (see

Table **2**).

Id. colour	N. molecules	Distance (Å)	E_ele	E_pol	E_dis	E_rep	E_tot
	1	24.10	-0.5	-0.0	-3.4	1.7	-2.5
	1	3.63	-28.6	-6.4	-171.3	117.1	-111.8
	1	10.57	-17.1	-5.2	-39.8	36.3	-34.1
	1	10.82	-5.0	-2.1	-14.3	2.3	-17.8
	1	17.94	-9.5	-2.7	-19.9	30.4	-10.5
	1	17.44	-0.7	-0.6	-8.3	2.3	-7.0
	1	22.35	-2.4	-0.0	-6.2	8.4	-2.7
	2	22.96	-0.4	-0.0	-5.0	0.8	-4.3
	1	23.65	-0.3	-0.0	-6.3	1.4	-5.0
	1	9.91	-18.5	-6.0	-41.6	35.6	-38.2

	1	7.26	-3.5	-0.2	-30.6	16.2	-20.5
	1	11.62	-1.0	-0.1	-2.5	0.0	-3.4
	1	19.51	0.1	-0.0	-0.6	0.0	-0.4
	1	4.42	-12.7	-2.9	-176.2	98.4	-108.2
	2	12.31	-0.7	-0.5	-12.7	1.7	-11.1
	1	11.20	-19.3	-7.5	-46.0	42.5	-39.8
	1	17.41	-0.3	-0.0	-0.5	0.0	-0.7
	1	17.02	-0.2	-0.0	-1.3	0.0	-1.3
	1	22.33	-0.2	-0.0	-0.5	0.0	-0.6
	1	18.13	-0.2	-0.0	-0.3	0.0	-0.5
	1	18.20	0.2	-0.0	-1.1	0.0	-0.7
	1	25.71	-0.1	-0.0	-2.0	0.1	-1.8
	1	21.57	-0.2	-0.0	-0.7	0.0	-0.8
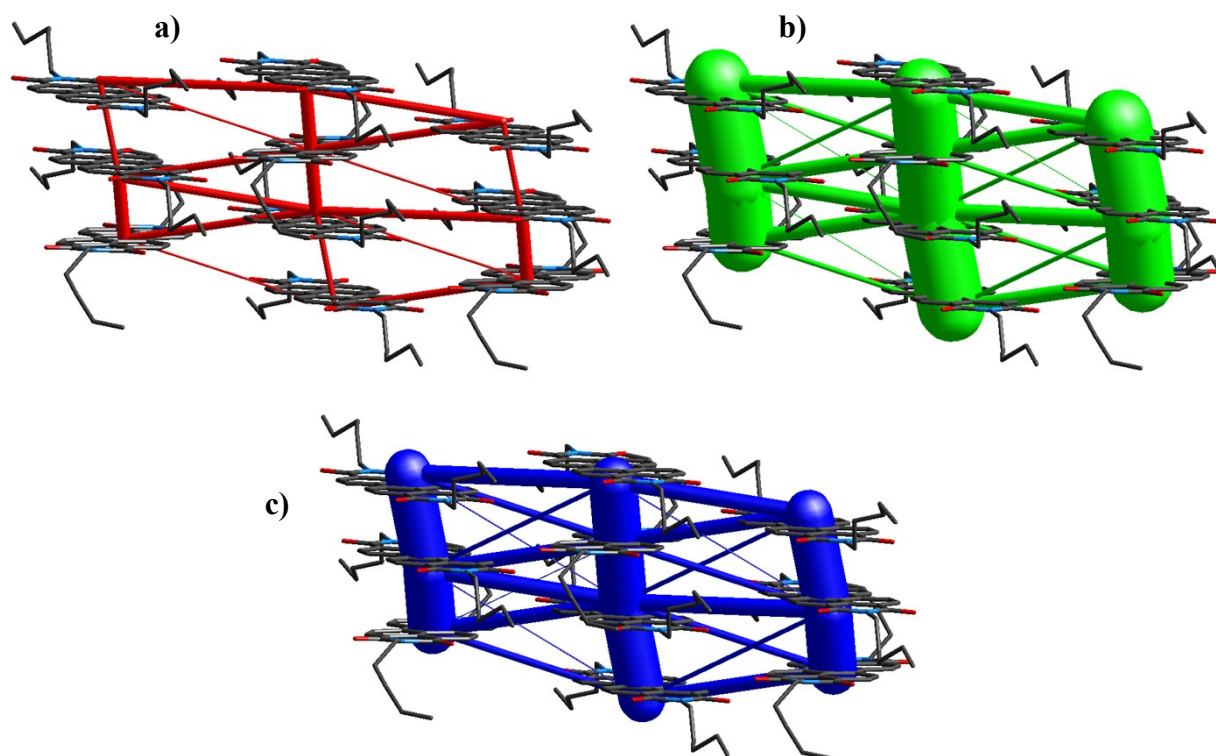
Figure S12. Graphic representation of the energy framework in PDI-C$_5$ form III calculated with CystalExplorer. The thickness of the lines is directly correlated with the intensity of the interaction. (a) electrostatic energy framework (red); (b) dispersion energy framework (green); (c) total energy framework (blue).
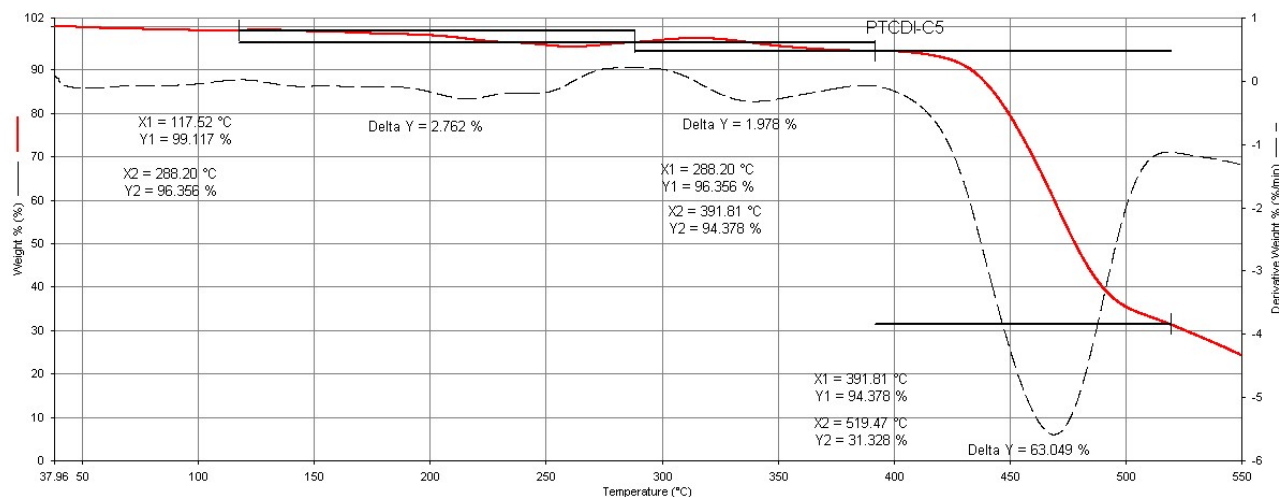
Thermogravimetrical analysis (TGA)

Figure S13. Thermogravimetrical analysis of PDI-C$_5$ in the temperature range RT – 550°C.

The TGA curve shows that the compound is thermally stable up to 400°C, then one weight loss step is observed.
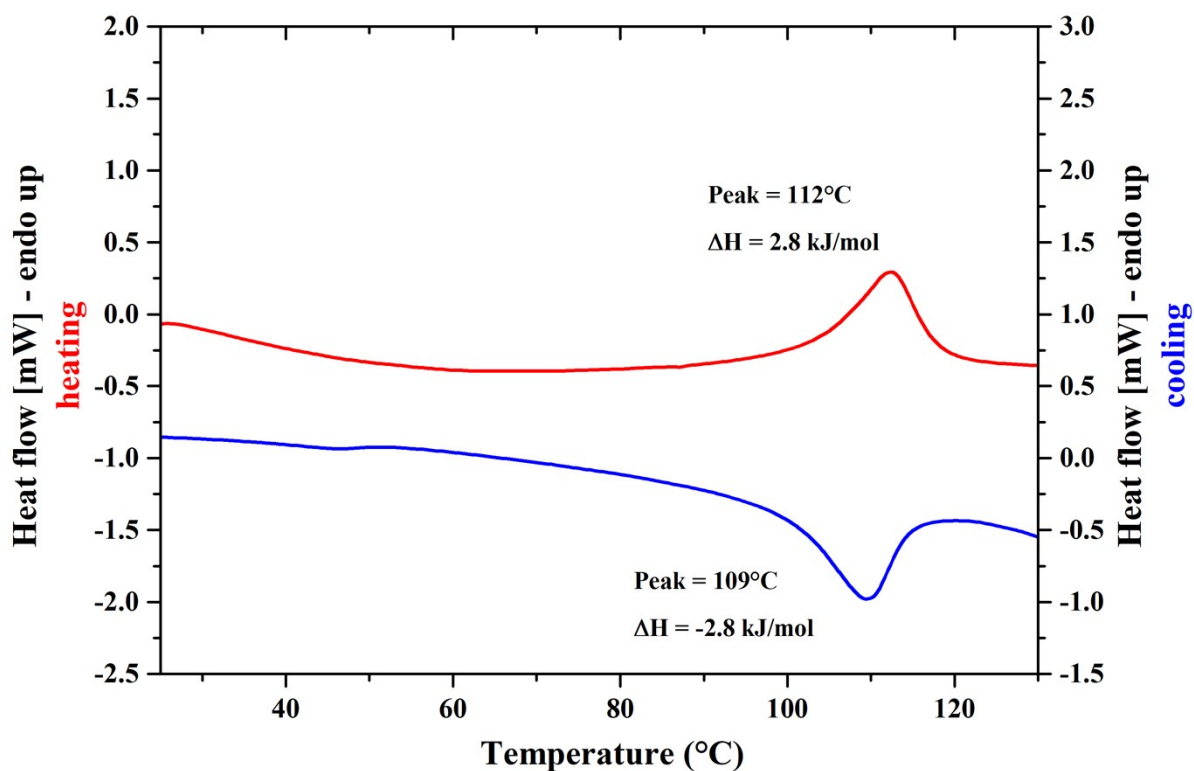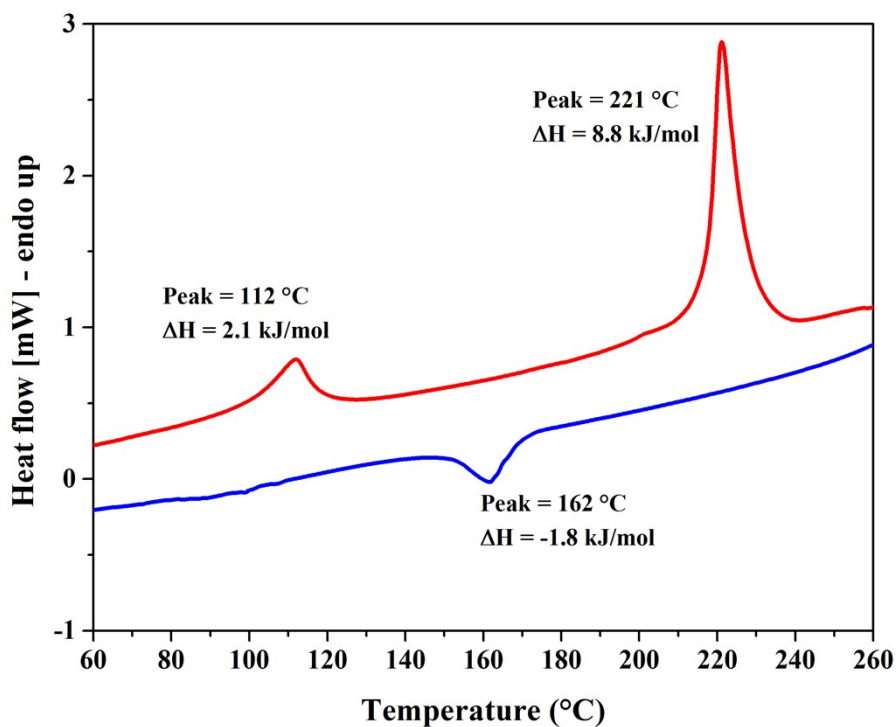
Differential Scanning Calorimetry (DSC)

Figure S14. Differential Scanning Calorimetry of PDI-C$_5$, measured in the temperature range RT - 140 °C with a 20 °C/min heating rate, in both heating (red curve) and cooling (blue curve). An endothermic event is observed in heating at 112 °C, while an exothermic event is observed at 109 °C upon cooling with the same DH of transition, indicating that this transition is fully reversible.

Figure S15. Differential Scanning Calorimetry of PDI-C_5, measured in the temperature range RT - 280 °C with a 20 °C/min heating rate, in both cooling and heating. Two endothermic events are observed in heating with peak at 112 and 221 °C respectively, while only one exothermic event is observed at 162 °C upon cooling.

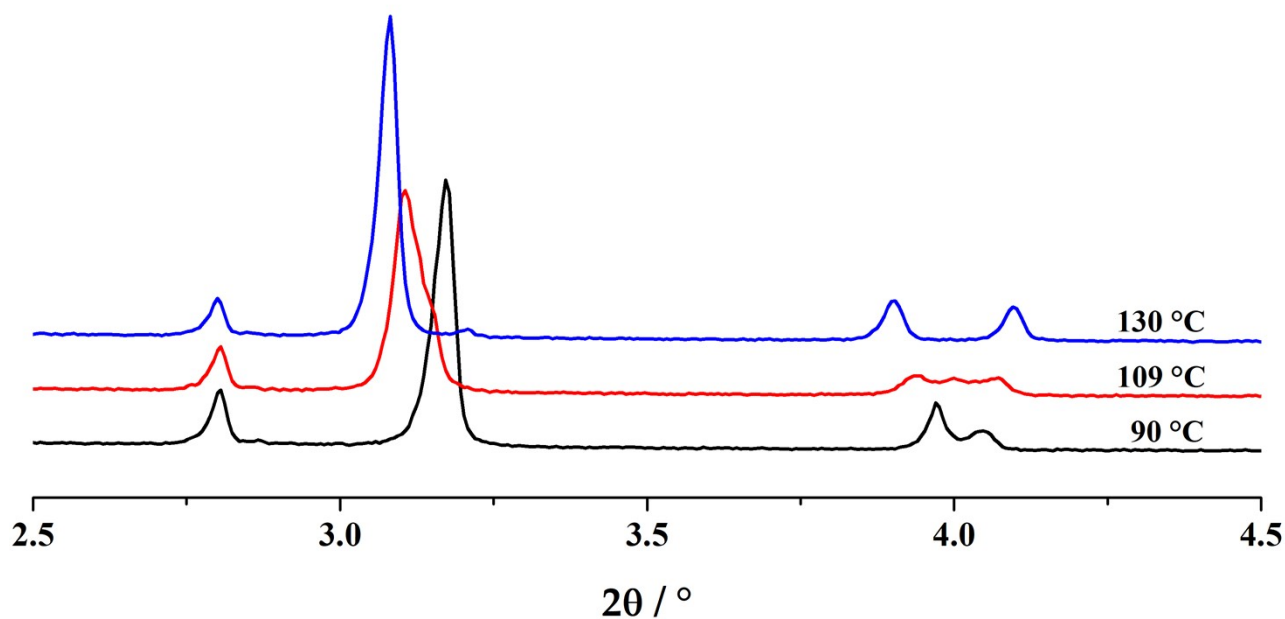## Variable Temperature X-ray Powder Diffraction (VTXRPD)

Figure S16. Variable temperature X-ray powder diffraction patterns of the material in the temperature range of the transition I-II. At 90 °C only form I is present (black); at 109 °C a mixture of form I and II is present (in red); at 130 °C all form I converted to form II.
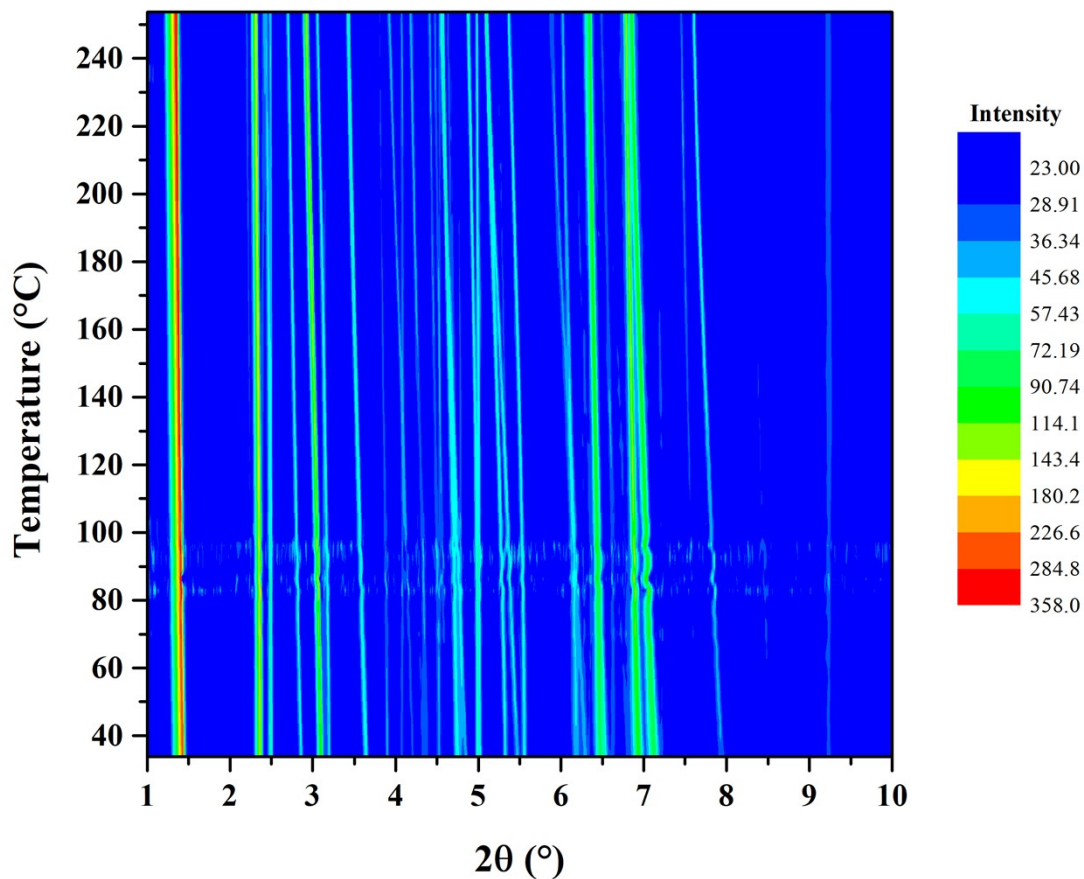
Figure S17. VTXRPD experiment of PDI-C$_5$ upon cooling. No changes that could be linked to phase transition are observed, indicating that form III was isolated at room temperature. Intensity is plotted in square root scale for clearness's sake.

Sequential Rietveld refinement was carried out using VTXRD data of the three separate forms. The sequential Rietveld refinement was performed according to the method described in the Durham Topas tutorial on "Sequential Rietveld Refinement of Multiple Data Sets". The variation of the crystal structure parameters of the three forms with temperature obtained by this method is reported here. Furthermore, the variation of the alkyl chain torsion angles with increasing temperature is reported for form I and form II, showing the different alkyl chain conformation.
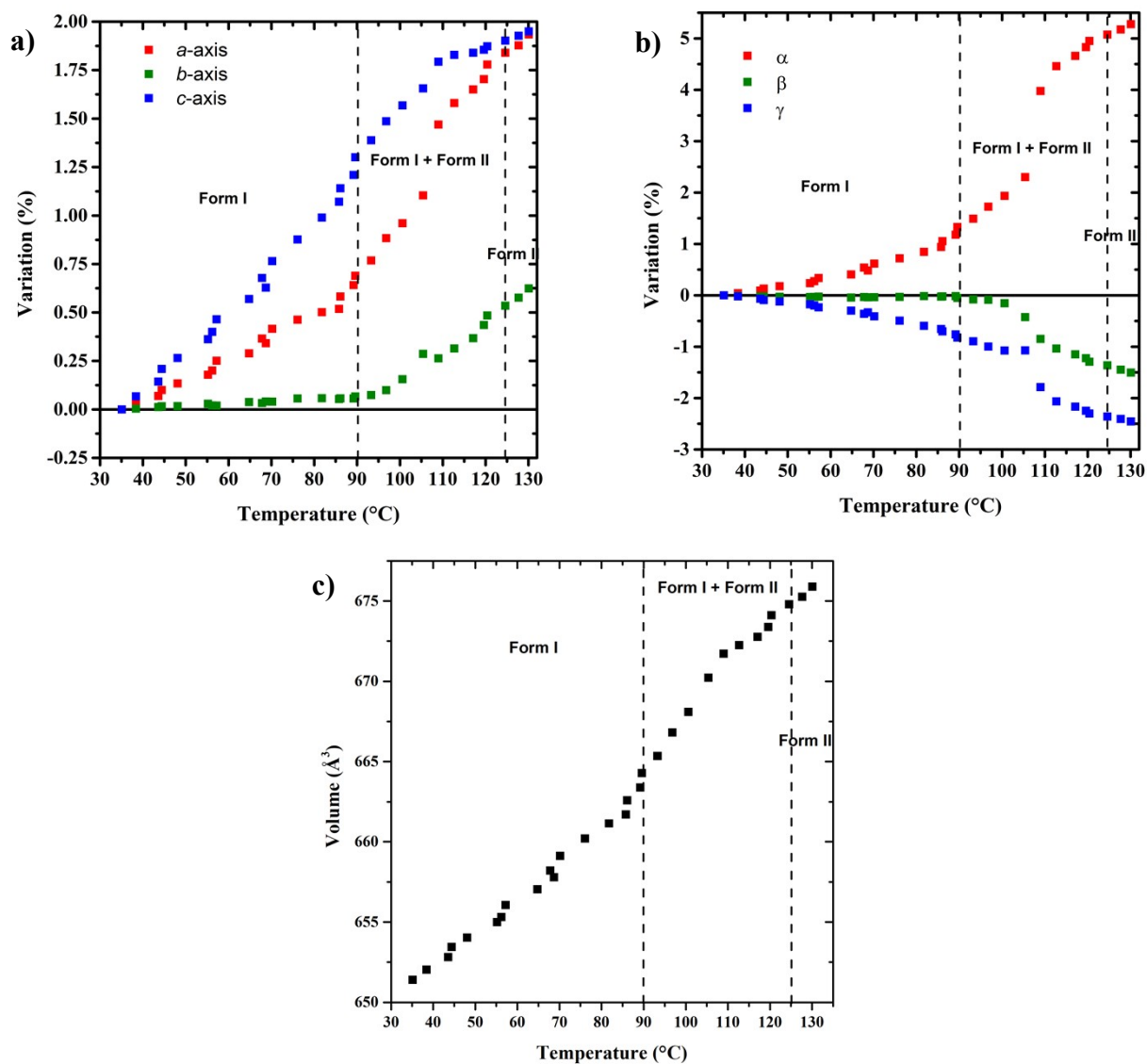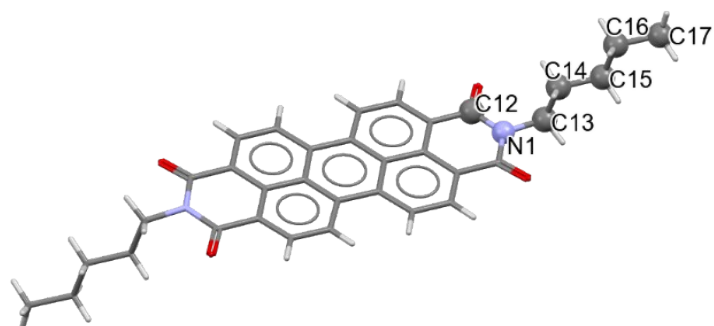
Figure S18. Sequential Rietveld refinement of PDI-C$_5$ form I, variation of unit cell parameters in the temperature range 35 – 130 °C. a) Variation in percentage of unit cell a-axis (red), b-axis (green) and c-axis (blue) with T; b) Variation in percentage of unit cell α (red), β (green) and γ (blue) angles with T; c) Variation of volume with T. The discontinuity in the trend of unit cell parameter with temperature, which indicates the transition to form II, is observed in the temperature range 90 – 125 °C (highlighted by the dashed lines).

The variation of the alkyl chain conformation with temperature in form I and II was reported using four torsion angles (see Figure S19).

Torsion 1 = C12-N1-C13-C14

Torsion 2 = N1-C13-C14-C15

Torsion 3 = C13-C14-C15-C16

Torsion 4 = C14-C15-C16-C17

Figure S19. Torsion angles used to describe alkyl chain conformation at different temperatures.
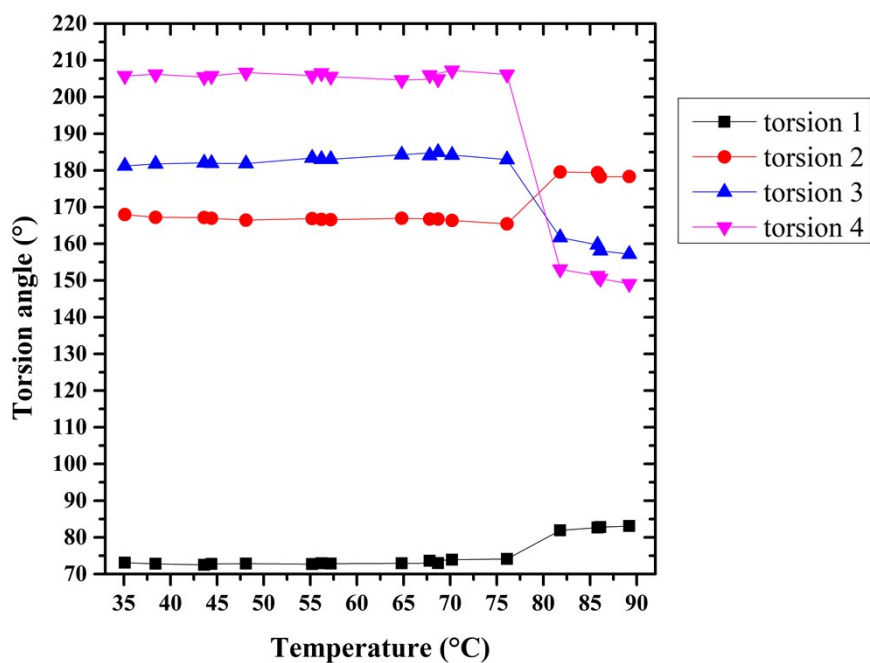

Figure S20. Variation of torsion angles of PDI-C5 form I alkyl chains with temperatures in the rang 35-90 °C. The four torsion angles change only slightly up to 75 °C, and after that temperature a drastic change is observed in all the torsion angles.
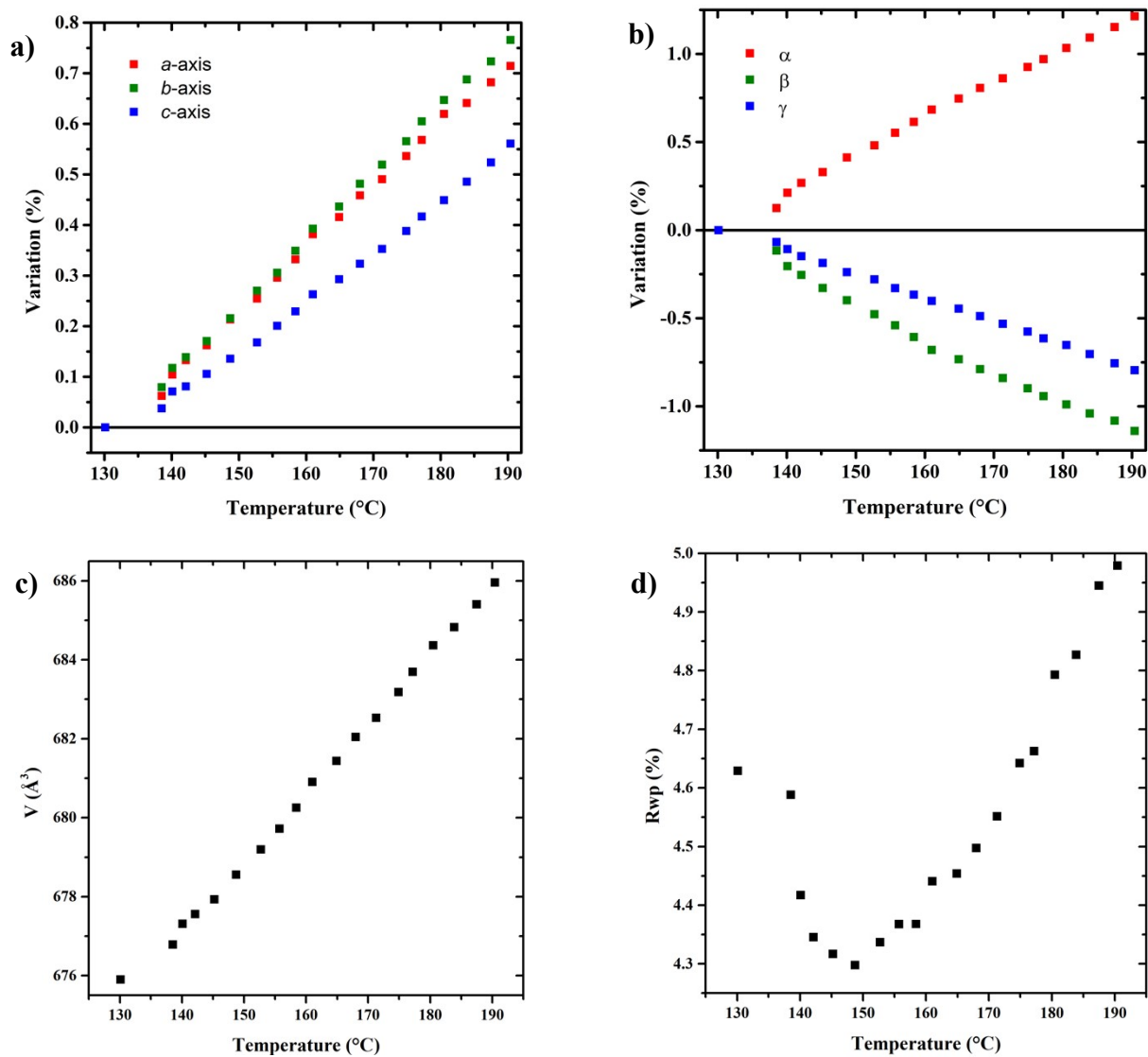
Figure S21. Sequential Rietveld refinement of PDI-C₅ form II, variation of unit cell parameters in the temperature range 130 – 190 °C. a) Variation in percentage of unit cell a-axis (red), b-axis (green) and c-axis (blue) with T; b) Variation in percentage of unit cell α (red), β (green) and γ (blue) angles with T; c) Variation of volume with T; d) Variation of R$_{wp}$ with T.
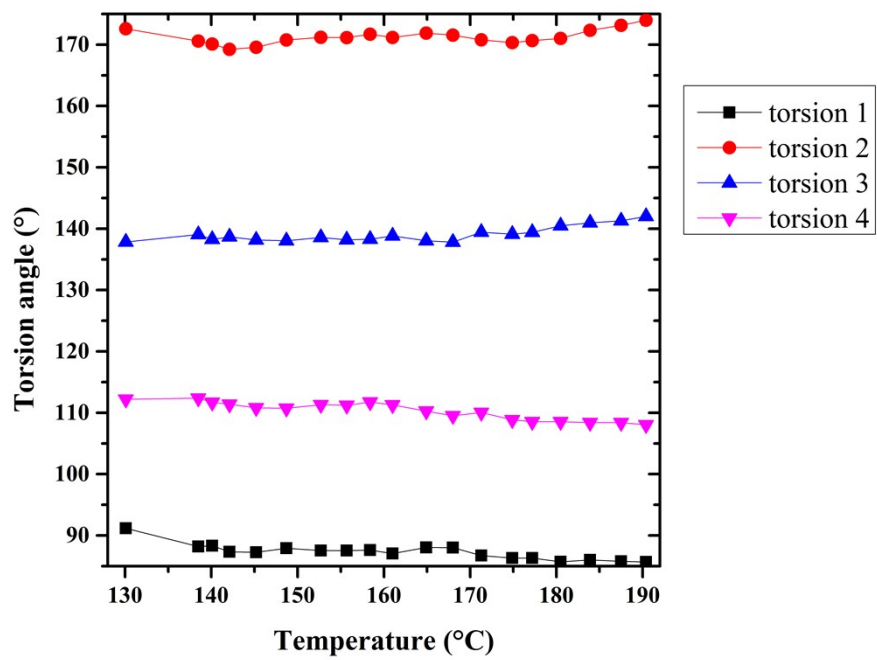
Figure S22. Variation of torsion angles of PDI-C$_5$ form II alkyl chains with temperatures in the range 130-190 °C. The four torsion angles change only slightly in the whole temperature range considered. The torsion angles are labelled as in Figure S19.
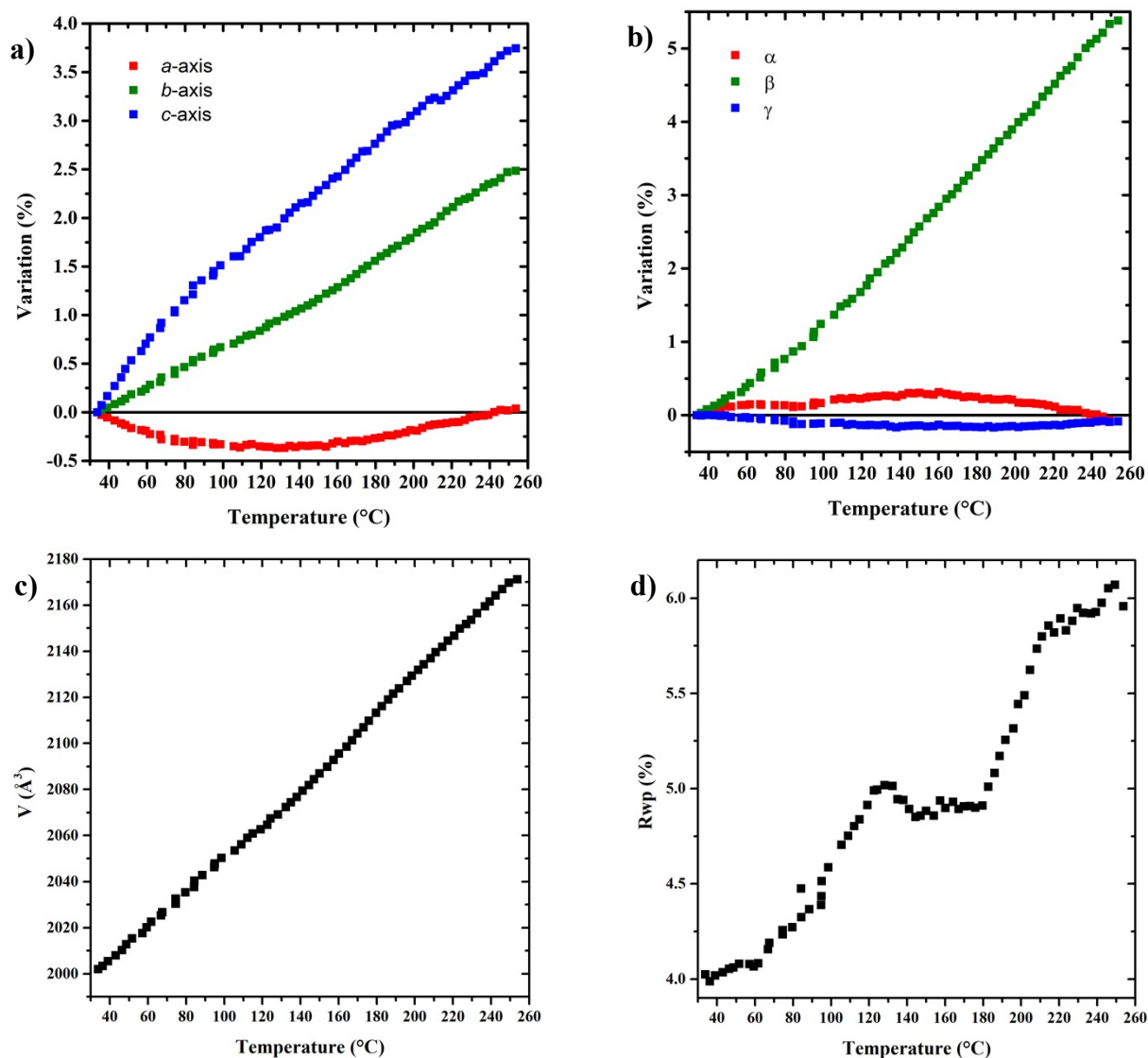
Figure S23. Sequential Rietveld refinement of PDI-C$_5$ form II, variation of unit cell parameters in the temperature range 35-225 °C. The VTXRPD data collected upon cooling form III to room temperature were used for this refinement. a) Variation in percentage of unit cell a-axis (red), b-axis (green) and c-axis (blue) with T; b) Variation in percentage of unit cell α (red), β (green) and γ (blue) angles with T; c) Variation of volume with T; d) Variation of R$_{wp}$ with T.

Thermal Expansion

The variation of unit cell parameters with temperature of the three forms were used to investigate their thermal expansion. The variation of the three principal axes with temperature is reported for the three forms, showing that in the temperature range considered the linear approximation holds.
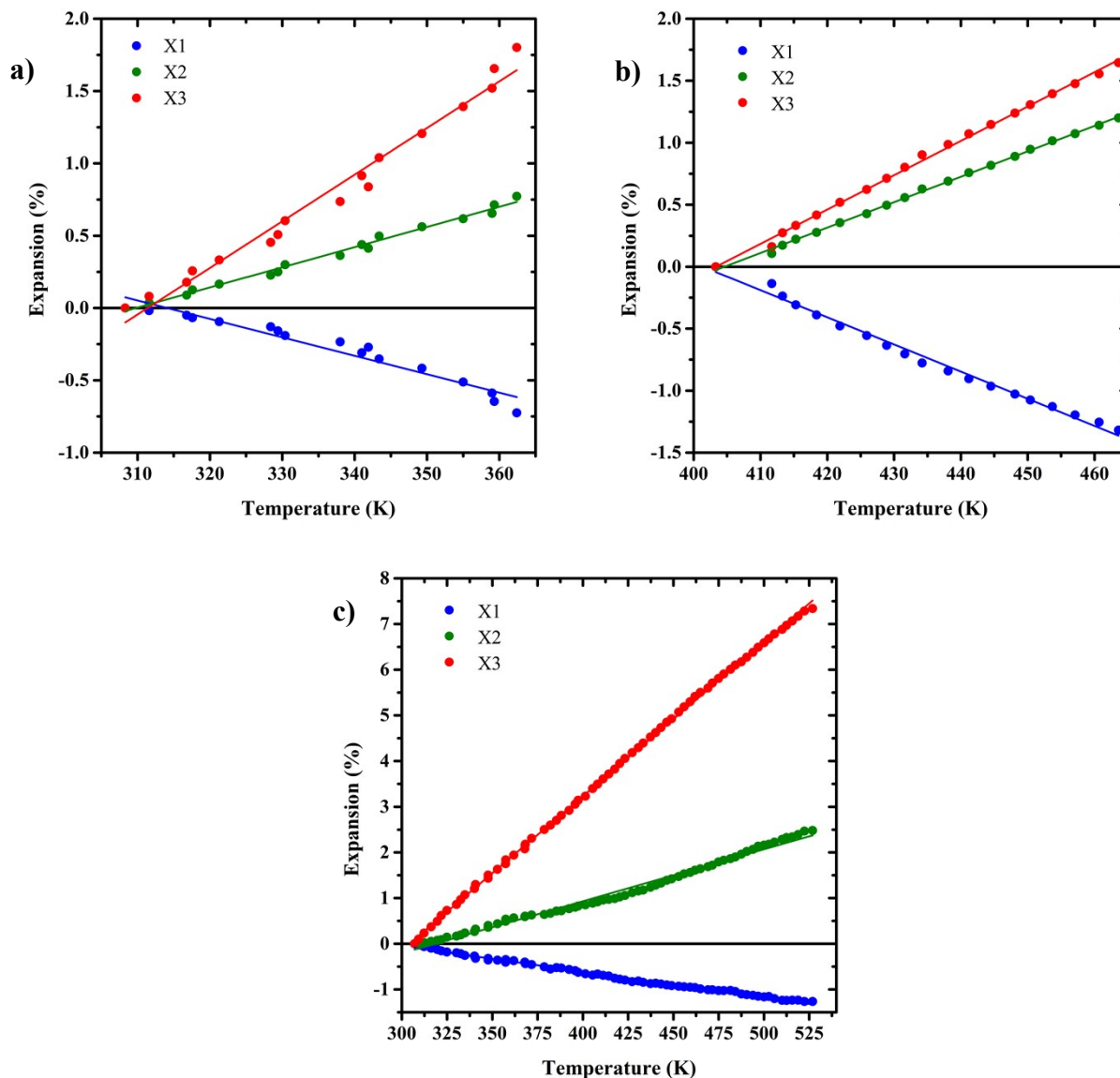
Figure S24. Variation (%) of the three principal axes X_1 (in blue), X_2 (in green), and X_3 (in red) with temperature in the three forms: a) form I; b) form II; c) form III. The linear approximation holds in the temperature range considered.

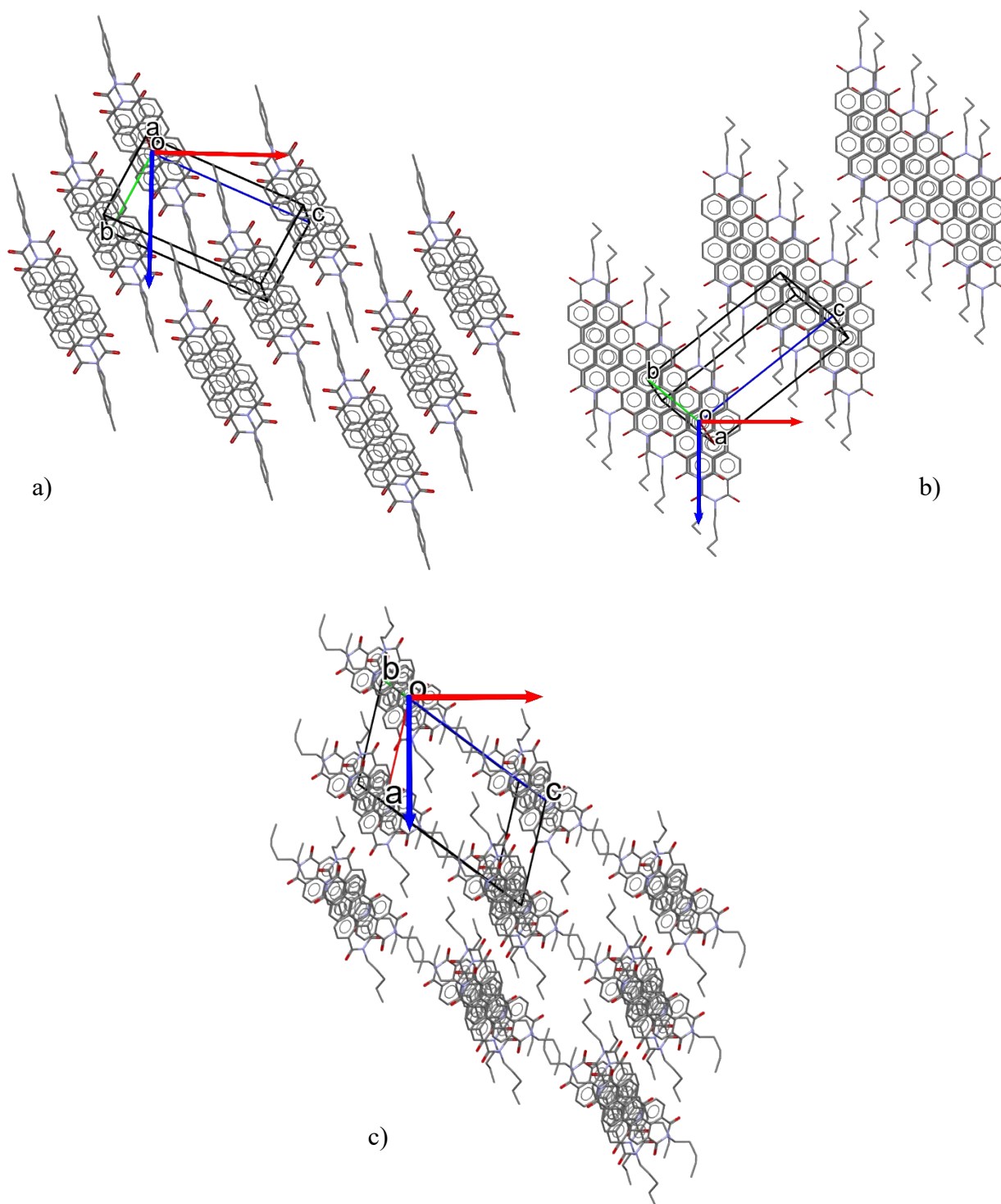The orientation of the principal axes within the structure is reported in Figure S25.

Figure S25. Packing of the structures a) form I, b) form II and c) form III with indicated the orientation of the thermal expansion principal axes calculated by PASCal: X_2 is perpendicular to the figure, while X_1 is indicated by the blue arrow and X_3 is indicated by the red arrow.
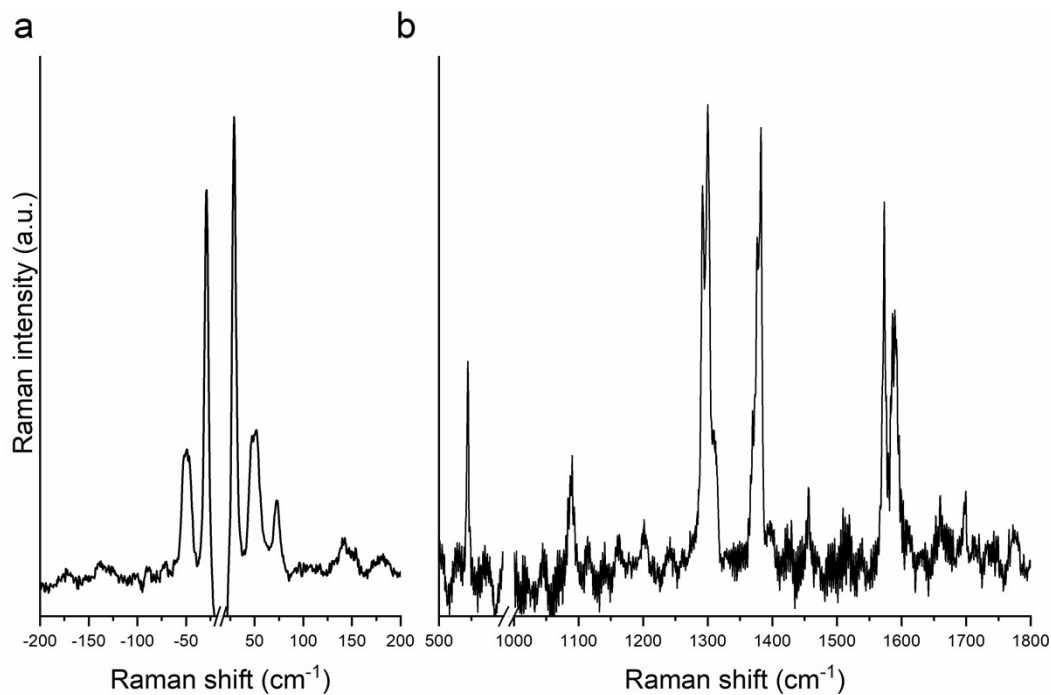
Raman Spectroscopy

Figure S26. Raman spectra at room temperature of PDI-C$_5$ in the low frequency range (a) showing Stokes and anti-Stokes peaks and in the high frequency range (b).
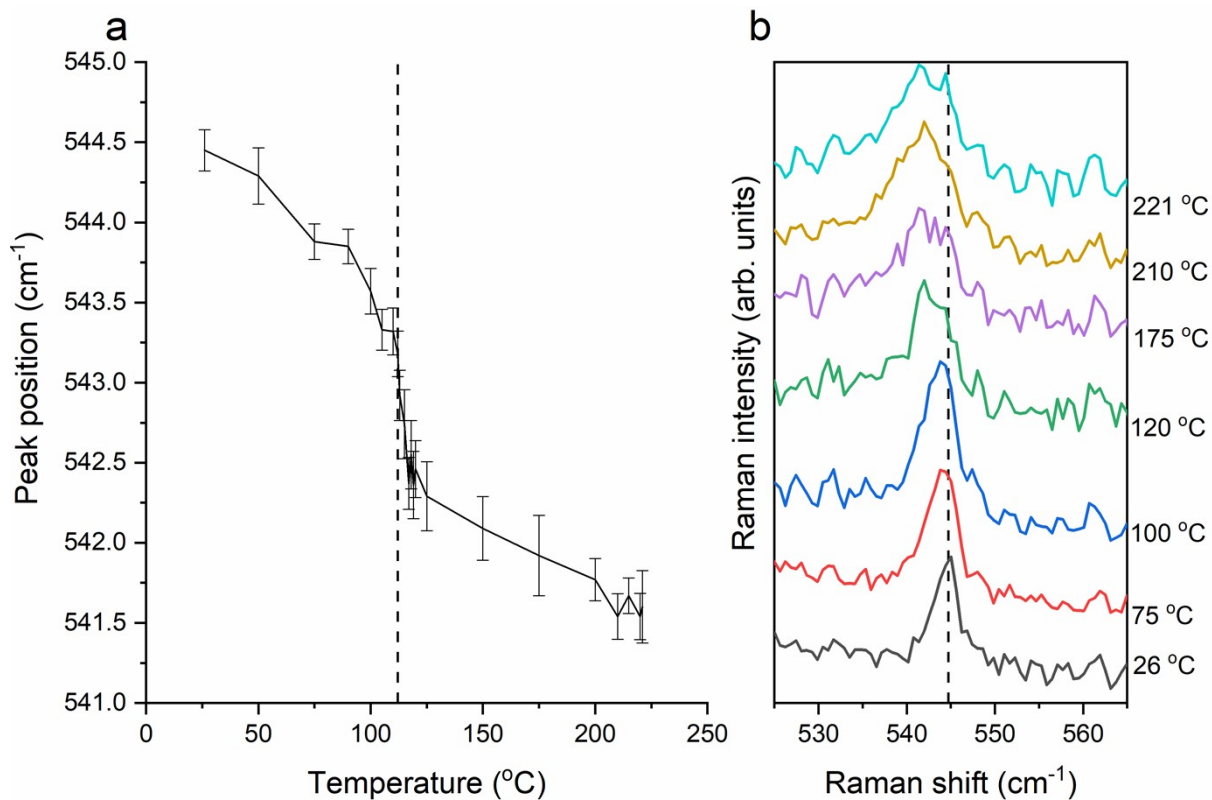

Figure S27. Intramolecular peak position as a function of the temperature (a) and corresponding Raman spectra (b).
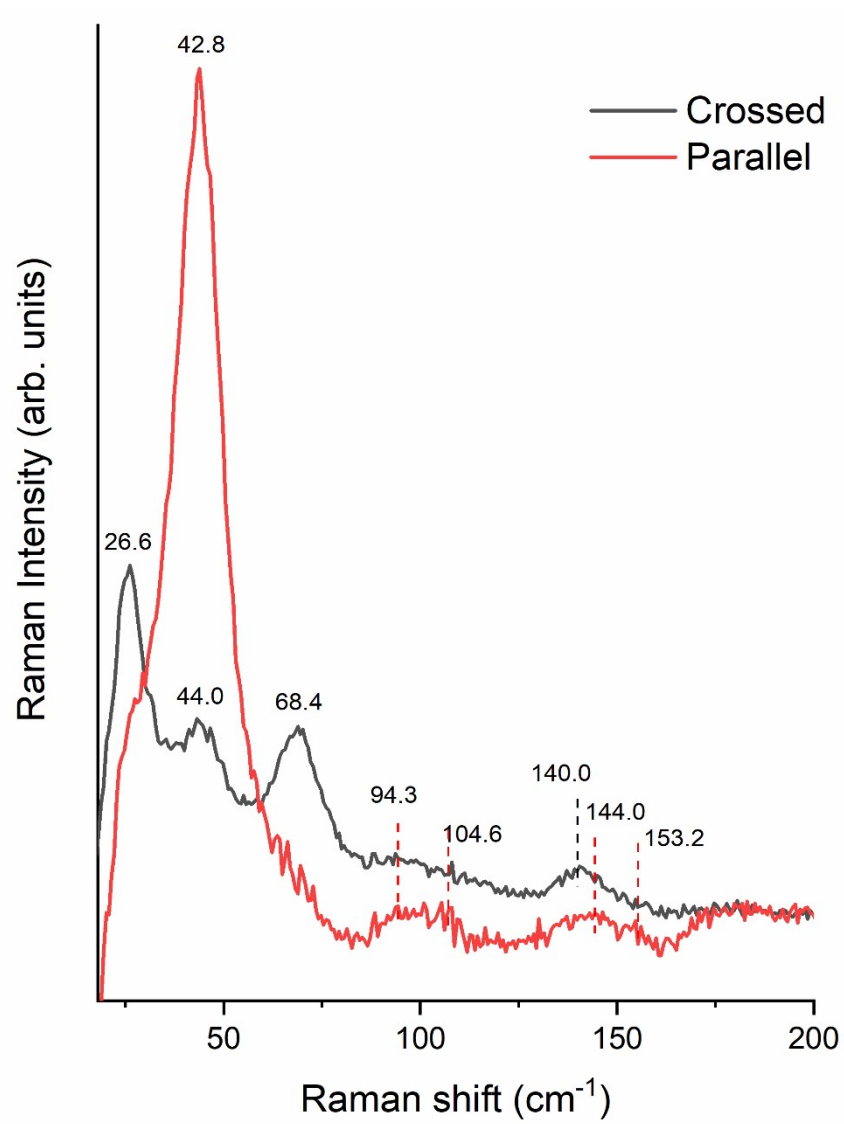
Figure S28. Polarized Low-frequency spectra of PDI-C$_5$ form III.